electricity

MDPI

Article

Optimal Transmission Switching and Grid Reconfiguration for Transmission Systems via Convex Relaxations

Vineet Jagadeesan Nair

Department of Mechanical Engineering, Massachusetts Institute of Technology, Cambridge, MA 02139, USA; jvineet9@mit.edu

Abstract

In this paper, we formulate optimization problems and successive convex relaxations to perform optimal transmission switching (OTS) in order to operate power transmission grids more efficiently. OTS may be crucial in future power grids with much higher penetrations of renewable energy sources, which will introduce more variability and intermittency in generation. Similarly, OTS can potentially help mitigate the effects of unpredictable demand fluctuations (e.g., due to extreme weather). We explore and compare several different formulations for the OTS problem in terms of the computational performance and optimality. In particular, we build upon the literature by considering more complex and accurate power flow formulations for OTS and introducing novel convex relaxations. This allows us to model the grid physics more accurately than prior works and generalize to several different types of networks. We also apply our methods to small transmission test cases as a proof of concept to determine the effects of applying OTS.

Keywords: power grids; smart grids; optimization; power flow

Academic Editor: Murilo E. C. Bento

Received: 18 February 2025
Revised: 22 June 2025
Accepted: 24 June 2025
Published: 3 July 2025

Citation: Jagadeesan Nair, V. Optimal Transmission Switching and Grid Reconfiguration for Transmission Systems via Convex Relaxations. *Electricity* **2025**, *6*, 37. https://doi.org/10.3390/electricity6030037

1. Introduction

Rapid decarbonization of the power grid is crucial to reduce greenhouse gas emissions and mitigate climate change. This will entail a transition away from centralized power generation sources like coal and natural gas to renewable sources like solar and wind. There will also be an increased footprint of batteries and other energy storage resources to help balance supply and demand. Furthermore, we are experiencing exponential load growth due to the increasing penetration of electric vehicles, heat pumps, and data centers. All of these changes place significant stress on the grid, resulting in long interconnection queues [1], congestion, and high curtailment of renewable resources. The aging grid infrastructure lacks adequate capacity to accommodate such increases in load and generation. Capacity additions, upgrades, and retrofits are also capital-intensive and often take 10+ years, with numerous regulatory barriers and permission issues, especially in the United States. Thus, grid modernization technologies are an attractive alternative to maximize the utilization of the existing grid capacity. These use real-time monitoring, optimization, and control to improve network operation without new physical investments. In a prior work, we studied the impacts of one such technology, i.e., dynamic line ratings, on the Texas grid [2]. In this work, we consider another such smart grid technology, optimal transmission switching (OTS).

In any given electrical network, several of the transmission lines are generally equipped with switches, circuit breakers, and/or reclosers. The conventional practice is to operate the grid using a static or fixed configuration. However, it may be beneficial to

dynamically reconfigure the grid through switching actions in order to respond to real-time demand and supply conditions. This has the potential to help reduce costs and improve efficiency. OTS is a grid reconfiguration method that dynamically opens or closes switches, circuit breakers, or reclosers to change the network topology in an optimal fashion [3]. This can be performed to achieve several different objectives, like minimizing electrical losses, generation costs, or congestion. In a highly decarbonized grid, this can help grid operators and utilities adapt to changing system conditions to avoid renewables curtailment and minimize the dispatch of natural gas peaker plants.

Prior Work and Contributions

There have been several previous works that have studied the impacts of OTS on transmission systems [4,5]. The majority of these works have relied on simplified direct current (DC)-based power flow models [3,6–9] or have used power transfer distribution factors (PTDFs) [10], thus resulting in mixed integer linear programs (MILPs). However, DC power flow solutions based on linearized approximation may not always be feasible in reality since they do not capture all constraints. Thus, it is preferable to use models that result in guaranteed feasible solutions.

A few works have applied alternating current (AC) power flow models to OTS [11,12], which resulted in mixed integer nonlinear programs (MINLPS). A subset of these papers modeled OTS problems as integer second-order cone programs [13,14]. Another class of papers included non-deterministic aspects through security constraints and contingencies [14], employing techniques like stochastic programming [15,16], robust optimization [17], and probabilistic analyses [18]. In order to improve computational traceability for larger networks, some have proposed simpler and faster heuristics for solving OTS [19,20], while sacrificing some optimality and risking potential infeasibilities. However, most of these papers still make some simplifying assumptions, restrict themselves to only certain types of networks, or ignore certain constraints completely, especially those relating to voltage angles. In this work, we aim to address this gap in the literature by incorporating all AC power flow constraints with convex relaxation strategies.

2. Optimal Power Flow Formulations for OTS

Optimal power flow is the key optimization problem that governs the operations of power systems. It describes the physical laws the system needs to obey, such as Kirchhoff's laws, Ohm's law, line thermal limits, etc. These are specified by the AC optimal power flow equations, shown below.

2.1. AC Optimal Power Flow

$$P_i + \mathbf{j}Q_i = V_i \sum_{k=1}^{n} \overline{\mathbf{Y}}_{ik} \bar{V}_k \tag{1}$$

Splitting these into real and imaginary components, we get

$$P_i = |V_i| \sum_{j=1}^{n} |V_j| \left(\mathbf{G}_{ij} \cos\left(\theta_i - \theta_j\right) + \mathbf{B}_{ij} \sin\left(\theta_i - \theta_j\right) \right), \tag{2}$$

$$Q_i = |V_i| \sum_{j=1}^{n} |V_j| \left(\mathbf{G}_{ij} \sin\left(\theta_i - \theta_j\right) - \mathbf{B}_{ij} \cos\left(\theta_i - \theta_j\right) \right). \tag{3}$$

These are clearly nonconvex constraints. Instead, a commonly used approach for transmission systems is to make several simplifying assumptions that result in the linear DC optimal power flow equations instead.

2.2. DC Optimal Power Flow

$$\min_{P_G, Q_G, |V|, \theta} \sum_{i \in \mathcal{G}} f_i(P_{Gi}), \tag{4}$$

subject to (5)

$$P_{Gi} - P_{Di} = \sum_{k=1}^{n} B_{ik}(\theta_i - \theta_k), \forall i \in N, \tag{6}$$

where k is the set of all nodes incident to node i (7)

$$P_{Gi}^{\min} \leq P_{Gi} \leq P_{Gi}^{\max}, \forall i \in G \tag{8}$$

$$-\overline{f}_{ik} \leq B_{ik}(\theta_i - \theta_k) \leq \overline{f}_{ik}, \forall (i,k) \in L \tag{9}$$

$$\theta_1 = 0 \quad \text{(Slack bus)} \tag{10}$$

$$|\theta_i - \theta_k| \leq \overline{\Delta\theta}_{ik}, \forall (i,k) \in L \tag{11}$$

These only account for the power balance (Equation (6)), generator capacities (Equation (8)), line power flow limits or thermal ratings (Equation (9)), and voltage angle constraints. While this is a reasonable approximation for high-voltage transmission grids with low line resistances, it has some key disadvantages since it completely ignores voltage magnitudes and reactive power. It also relies on a small-angle approximation to linearize all the trigonometric terms. Thus, it cannot be guaranteed that the DC-OPF solutions are feasible for the real ACOPF problem. Furthermore, the DC approximation is even worse for lower voltage distribution grids that have more losses (even though we are restricting ourselves to transmission systems in this paper).

2.3. DC OPF-Based OTS

Most of the studies in the literature have relied on an OTS problem formulation using DC OPF [3,7], resulting in modifying the power balance constraints in Equation (6) and line flow limits in Equation (9) accordingly, to indicate whether a line is open or closed:

$$P_{Gi} - P_{Di} - \sum_{k=1}^{n} (B_{ik}(\theta_i - \theta_k) + (1 - z_{ik})M) \geq 0, \forall i \in N \tag{12}$$

$$P_{Gi} - P_{Di} - \sum_{k=1}^{n} (B_{ik}(\theta_i - \theta_k) - (1 - z_{ik})M) \leq 0, \forall i \in N \tag{13}$$

$$-z_{ik}\overline{f}_{ik} \leq B_{ik}(\theta_i - \theta_k) \leq z_{ik}\overline{f}_{ik}, \forall (i,k) \in L \tag{14}$$

$$\sum_{k} (1 - z_k) \leq Z, \quad z_{ik} \in \{0,1\} \tag{15}$$

Here, the binary variable z indicates whether a line is open ($z_{ik} = 0$) and no power flows through it, or closed ($z_{ik} = 1$) and all the constraints apply to it.

2.4. Towards ACOPF-Based OTS Formulations

We can reformulate the AC OPF problem by introducing additional auxiliary variables to represent the nonlinear terms (see Table 1 for details) and transform them into the following [21–23]:

$$\min_{p,q,c,s,\theta} \sum_{i \in I} \sum_{i \in G} f_i(P_{Gi}) \tag{16}$$

$$\underline{p}_i^{\mathrm{G}} \leq p_i^{\mathrm{G}} \leq \bar{p}_i^{\mathrm{G}}, \quad i = 1, 2, \cdots, n \tag{17}$$

$$\underline{q}_i^{\mathrm{G}} \leq q_i^{\mathrm{G}} \leq \bar{q}_i^{\mathrm{G}}, \quad i = 1, 2, \cdots, n \tag{18}$$

$$\underline{V}_i^2 \leq e_i \leq \bar{V}_i^2, \quad i = 1, 2, \cdots, n \tag{19}$$

$$p_i^{\mathrm{G}} + p_i^{\mathrm{U}} - p_i^{\mathrm{D}} = G_{ii}e_i + \sum_{j=1, j\neq i}^{n} \left(G_{ij}c_{ij} + B_{ij}s_{ij}\right), \quad i = 1, 2, \cdots, n \tag{20}$$

$$q_i^{\mathrm{G}} + q_i^{\mathrm{U}} - q_i^{\mathrm{D}} = -B_{ii}e_i - \sum_{j=1, j\neq i}^{n} \left(B_{ij}c_{ij} - G_{ij}s_{ij}\right), \quad i = 1, 2, \cdots, n \tag{21}$$

$$\left(-G_{ij}e_i + G_{ij}c_{ij} + B_{ij}s_{ij}\right)^2 + \left(B_{ij}e_i - B_{ij}c_{ij} + G_{ij}s_{ij}\right)^2 \leq \left(\overline{f}_{ij}\right)^2 \forall (i,j) \in L \tag{22}$$

$$c_{ij}^2 + s_{ij}^2 = e_i e_j, \quad (i,j) \in L \tag{23}$$

$$\theta_i - \theta_j = \arctan\left(s_{ij}/c_{ij}\right) \forall (i,j) \in L \tag{24}$$

$$\underline{\Delta\theta} \leq \theta_i - \theta_j \leq \overline{\Delta\theta} \tag{25}$$

Table 1. Definitions of important variables and parameters.

Variable or Parameter	Definition
n	Number of buses or nodes in network
(i,j)	Bus indices
L	Set of all transmission line indices
$\mathcal{G}$	Set of all generators
a_{ij}	Binary variable indicating whether line ij is open or closed
θ_i	Voltage angle at bus i
$\theta_{ij} = \theta_i - \theta_j$	Voltage angle difference between buses i and j
V_i	Complex voltage at bus i
$\lvert V_i \rvert$	Voltage magnitude at bus i
c_{ij}	$= \lvert V_i \rvert \lvert V_j \rvert cos(\theta_{ij})$
s_{ij}	$= \lvert V_i \rvert \lvert V_j \rvert sin(\theta_{ij})$
e_i	$e_i = V_i^2$
Y_{ij}	Admittance matrix element of line ij
G_{ij}, B_{ij}	Real/reactive parts of admittance matrix element of line ij
G_{ii}, B_{ii}	Real/reactive parts of admittance matrix diagonal element of bus i
b_{ij}	Shunt susceptance of line ij
$\overline{f}_{ij}$	Apparent power flow capacity of line ij

We notice that now, most of the constraints are actually convex, except for Equations (23) and (24). Note that Equation (22) is already a convex quadratic second-order conic constraint. For the first constraint Equation (23), we first relax the equality to the following inequality:

$$c_{ij}^2 + s_{ij}^2 \leq e_i e_j \quad \forall (i,j) \in L;$$

then, this can be transformed into a convex quadratic second-order cone programming (SOCP) constraint by defining additional auxiliary variables D_{ij}^{1-4} in order to represent the bilinear right-hand side term. Thus, we can replace Equations (22) and (23) with the following set of constraints:

$$p_{ij} = -G_{ij}e_i + G_{ij}c_{ij} + B_{ij}s_{ij}, \quad \forall (i,j) \in L \tag{26}$$

$$q_{ij} = \left(B_{ij} - b_{ij}/2\right)e_i - B_{ij}c_{ij} + G_{ij}s_{ij}, \quad \forall (i,j) \in L \tag{27}$$

$$\left(p_{ij}\right)^2 + \left(q_{ij}\right)^2 \leq \left(\overline{f}_{ij}\right)^2, \quad \forall (i,j) \in L \tag{28}$$

$$D_{ij}^1 = 2c_{ij}, \quad \forall (i,j) \in L \tag{29}$$

$$D_{ij}^2 = 2s_{ij}, \quad \forall (i,j) \in L \tag{30}$$

$$D_{ij}^3 = e_i - e_j, \quad \forall (i,j) \in L \tag{31}$$

$$D_{ij}^4 = e_i + e_j, \quad \forall (i,j) \in L \tag{32}$$

$$\left(D_{ij}^{1}\right)^{2}+\left(D_{ij}^{2}\right)^{2}+\left(D_{ij}^{3}\right)^{2}\leq\left(D_{ij}^{4}\right)^{2},\quad\forall(i,j)\in L \tag{33}$$

We chose to employ a second-order conic relaxation (SOCP) here as opposed to a semidefinite programming relaxation (SDP). Although SDP relaxations have been proven to be exact for certain types of radial networks, they tend to perform poorly in practice and worse than SOCP, especially for larger problems [24,25]. We expect to see similar trends with SDP in our case as well—while it may produce more accurate results with a smaller optimality gap, it would be less computationally efficient, resulting in longer runtimes [26,27]. Thus, we decided to focus on using the SOCP approach, since it provides a better balance of accuracy and speed compared to the DCOPF (less accurate, faster solutions) and SDP-based AC OPF (more accurate, slower solutions). We use the SOCP formulation for the OTS problem by introducing binary decision variables for which transmission lines or branches to keep open. While a few other papers have considered applying ACOPF models for OTS, they also rely on quite restrictive assumptions and approximations as part of their final approach [4,12,13]. This motivates the goal behind this paper: to apply as accurate an OPF formulation as possible for the OTS problem.

2.5. Optimal Transmission Switching Problem

$$\min_{p,q,c,s,\theta}\sum_{i\in I}\sum_{i\in G}f_i(P_{Gi}) \tag{34}$$

$$\underline{p}_i^{G}\leq p_i^{G}\leq\bar{p}_i^{G},\quad i=1,2,\cdots,n \tag{35}$$

$$\underline{q}_i^{G}\leq q_i^{G}\leq\bar{q}_i^{G},\quad i=1,2,\cdots,n \tag{36}$$

$$\underline{V}_i^{2}\leq e_i\leq\bar{V}_i^{2},\quad i=1,2,\cdots,n \tag{37}$$

$$p_i^{G}-p_i^{D}=\sum_{j=1,j\neq i}^{n}p_{ij},\quad i=1,2,\cdots,n \tag{38}$$

$$q_i^{G}-q_i^{D}=\sum_{j=1,j\neq i}^{n}q_{ij},\quad i=1,2,\cdots,n \tag{39}$$

$$p_{ij}=a_{ij}\left(-G_{ij}e_i+G_{ij}c_{ij}+B_{ij}s_{ij}\right),\quad\forall(i,j)\in L \tag{40}$$

$$q_{ij}=a_{ij}\left(\left(B_{ij}-b_{ij}/2\right)e_i-B_{ij}c_{ij}+G_{ij}s_{ij}\right),\quad\forall(i,j)\in L \tag{41}$$

$$\theta_i-\theta_j=\arctan\left(s_{ij}/c_{ij}\right),\quad\forall(i,j)\in L \tag{42}$$

$$\left(p_{ij}\right)^{2}+\left(q_{ij}\right)^{2}\leq a_{ij}\left(\overline{f}_{ij}\right)^{2},\quad\forall(i,j)\in L \tag{43}$$

$$D_{ij}^{1}=2c_{ij},\quad\forall(i,j)\in L \tag{44}$$

$$D_{ij}^{2}=2s_{ij},\quad\forall(i,j)\in L \tag{45}$$

$$D_{ij}^{3}=e_i-e_j,\quad\forall(i,j)\in L \tag{46}$$

$$D_{ij}^{4}=e_i+e_j,\quad\forall(i,j)\in L \tag{47}$$

$$\left(D_{ij}^{1}\right)^{2}+\left(D_{ij}^{2}\right)^{2}+\left(D_{ij}^{3}\right)^{2}\leq\left(D_{ij}^{4}\right)^{2},\quad\forall(i,j)\in L \tag{48}$$

$$a_{ij}\in\{0,1\}\quad\forall(i,j)\in L \tag{49}$$

$$\underline{\Delta\theta}\leq\theta_i-\theta_j\leq\overline{\Delta\theta} \tag{50}$$

$$p,q,\theta\in\mathbb{R}^{n};\ c,s\in\mathbb{R}^{n\times n};\ a\in\mathbb{R}^{|L|} \tag{51}$$

This is a mixed integer nonlinear programming problem (MINLP), which is generally challenging to solve, especially as we consider large network sizes with many buses/nodes and branches. We thus focus on reformulating the problematic constraints. The nonconvex constraint Equation (42) is needed to uniquely define the voltage angles. Most prior papers

simply discard this constraint entirely—while this is a valid approach for radial networks, it cannot be ignored for more general meshed networks, which are the dominant topology for transmission systems. In order to convexify this, we first rewrite this constraint as follows:

$$\theta_{ij} = \theta_i - \theta_j = \tan^{-1}(s_{ij}/c_{ij}) \implies \tan(\theta_{ij}) = (s_{ij}/c_{ij}).$$

For the stable operation of power systems, the voltage angle difference between neighboring buses needs to be kept small, e.g., $-1.047 = \underline{\Delta\theta} \leq \theta_{ij} \leq \overline{\Delta\theta} = 1.047$ rad. The bus voltage angle differences are small. For instance, voltage differences between buses are generally maintained at less than 10° [28] in steady state, with the maximum angle differences generally lying between 5 and 20° under normal operating conditions [29,30]. However, note that for certain large inter-area systems, these can sometimes reach 60° [31]. We focus only on radial and meshed networks in this paper, since they are the most common types of transmission networks. While ring networks may have larger angle differences, these are not very common in practice and are mainly relevant only for urban distribution grids and medium-voltage systems [32].

Thus, for most general transmission networks, we can apply a small-angle approximation for $\tan()$ to relax this constraint:

$$\lim_{\theta \to 0} \frac{\tan(\theta)}{\theta} = 1.$$

Thus, the nonconvex constraint Equation (24) can be reduced to the following bilinear equality constraint:

$$\theta_i - \theta_j = \frac{s_{ij}}{c_{ij}} \implies s_{ij} = c_{ij}\theta_{ij}.$$

This can further be relaxed by employing McCormick envelope (MCE) convex relaxations, replacing this bilinear term with a series of linear inequality constraints. We know

$$\begin{aligned}
&-|\overline{V}_i||\overline{V}_j| \leq s_{ij} = |V_i||V_j|sin(\theta_{ij}) \leq |\overline{V}_i||\overline{V}_j| \\
&-|\overline{V}_i||\overline{V}_j| \leq c_{ij} = |V_i||V_j|cos(\theta_{ij}) \leq |\overline{V}_i||\overline{V}_j| \\
&\because -1 \leq sin(\theta_{ij}), cos(\theta_{ij}). \leq 1
\end{aligned}$$

Generally, we aim to maintain all bus voltages within a tight interval as close to 1 p.u. as possible, e.g., $0.9 = |\underline{V}|$ p.u. $\leq |V_i| \leq |\overline{V}| = 1.1$ p.u. This allows us to bound both $c_{ij}, s_{ij} \in \left[-|\overline{V}|^2, |\overline{V}|^2\right]$ and furthermore $\theta_{ij} \in \left[\underline{\Delta\theta}, \overline{\Delta\theta}\right]$. We can narrow the bounds for c_{ij} further to $|\underline{c}_{ij}, \overline{c}_{ij}| = |\overline{V}|^2 cos(\underline{\Delta\theta}) \leq c_{ij} \leq |\overline{V}|^2$ ($\because 0 \in \left[\underline{\Delta\theta}, \overline{\Delta\theta}\right]$). Thus, we can construct the McCormick envelopes by replacing the bilinear term with an auxiliary variable $w_{ij} = c_{ij}\theta_{ij}$ with the following associated constraints:

$$w_{ij} \geq \underline{c}_{ij}\theta_{ij} + c_{ij}\underline{\theta}_{ij} - \underline{c}_{ij}\underline{\theta}_{ij} \tag{52}$$

$$w_{ij} \geq \overline{c}_{ij}\theta_{ij} + c_{ij}\overline{\theta}_{ij} - \overline{c}_{ij}\overline{\theta}_{ij} \tag{53}$$

$$w_{ij} \leq \overline{c}_{ij}\theta_{ij} + c_{ij}\underline{\theta}_{ij} - \overline{c}_{ij}\underline{\theta}_{ij} \tag{54}$$

$$w_{ij} \leq c_{ij}\overline{\theta}_{ij} + \underline{c}_{ij}\theta_{ij} - \underline{c}_{ij}\overline{\theta}_{ij}. \tag{55}$$

Note that we only focus on OTS under nominal or normal operating conditions, for which the $[0.9, 1.1]$ p.u. range of voltage magnitudes is well within the $\pm 5\%$ limits set by the American National Standards Institute (ANSI) [33]. Voltages may exceed $\pm 10\%$ for short periods during disturbances like line faults or load swings, but such contingency conditions are outside the scope of this work. Of course, the tightness of this MCE relaxation depends heavily on the variable bounds used to construct the convex underestimators and concave overestimators. The relaxation could be improved further by iteratively decreasing

the upper bounds and increasing the lower bounds, through piecewise MCE relaxations or other similar approaches [34].

In our case, we note that we can obtain even tighter bounds on c_{ij} by noting that $-1.047 = \underline{\Delta\theta} \leq \theta_{ij} \leq \overline{\Delta\theta} = 1.047\ rad$, and $cos(1.047) \approx \frac{1}{2} \leq cos(\theta) \leq 1$ for $\theta \in [-1.047, 1.047]$. This implies that $\frac{|\overline{V}|^2}{2} \leq c_{ij} \leq |\overline{V}|^2$. Plugging these into Equations (52)–(55) gives us

$$\begin{aligned} w_{ij} &\geq \frac{|\overline{V}|^2\theta_{ij}}{2} + c_{ij}\underline{\Delta\theta} - \frac{|\overline{V}|^2\underline{\Delta\theta}}{2} \\ w_{ij} &\geq |\overline{V}|^2\theta_{ij} + c_{ij}\overline{\Delta\theta} - |\overline{V}|^2\overline{\Delta\theta} \\ w_{ij} &\leq |\overline{V}|^2\theta_{ij} + c_{ij}\underline{\Delta\theta} - |\overline{V}|^2\underline{\Delta\theta} \\ w_{ij} &\leq c_{ij}\overline{\Delta\theta} + \frac{|\overline{V}|^2\theta_{ij}}{2} - \frac{|\overline{V}|^2\overline{\Delta\theta}}{2}. \end{aligned}$$

Disjunctive or Conditional Constraints

We introduce additional binary variables $a_{ij} \in \{0, 1\}$ for each line $ij \in L$ that indicates whether a line is open or closed. In order to represent switching, we need to enforce that both the real and reactive power flows on an open line are constrained to zero, since an open circuit cannot transfer any current. We thus need to modify the constraints Equations (40) and (41) accordingly:

$$p_{ij} = a_{ij}\big(-G_{ij}e_i + G_{ij}c_{ij} + B_{ij}s_{ij}\big), \quad \forall (i,j) \in L \tag{56}$$

$$q_{ij} = a_{ij}\big((B_{ij} - b_{ij}/2)e_i - B_{ij}c_{ij} + G_{ij}s_{ij}\big), \quad \forall (i,j) \in L. \tag{57}$$

Since we do not know the exact bounds on the continuous variables (terms inside the parentheses), an exact linear reformulation of this bilinear constraint is not possible. However, we can represent this using the following set of disjunctive or conditional equalities:

$$\begin{bmatrix} a_{ij} \\ p_{ij} = -G_{ij}e_i + G_{ij}c_{ij} + B_{ij}s_{ij} \\ q_{ij} = (B_{ij} - b_{ij}/2)e_i - B_{ij}c_{ij} + G_{ij}s_{ij} \end{bmatrix} \vee \begin{bmatrix} \neg a_{ij} \\ p_{ij} = 0 \\ q_{ij} = 0 \end{bmatrix}. \tag{58}$$

These can be relaxed to the following linear constraints using the big-M method, allowing us to get rid of the bilinear terms involving products of continuous and binary variables:

$$\begin{aligned} -p_{ij} - G_{ij}e_i + G_{ij}c_{ij} + B_{ij}s_{ij} + (1 - a_{ij})M_{ij} &\geq 0 \\ -p_{ij} - G_{ij}e_i + G_{ij}c_{ij} + B_{ij}s_{ij} - (1 - a_{ij})M_{ij} &\leq 0 \\ -q_{ij} + (B_{ij} - b_{ij}/2)e_i - B_{ij}c_{ij} + G_{ij}s_{ij} + (1 - a_{ij})N_{ij} &\geq 0 \\ -q_{ij} + (B_{ij} - b_{ij}/2)e_i - B_{ij}c_{ij} + G_{ij}s_{ij} - (1 - a_{ij})N_{ij} &\geq 0 \\ -M_{ij}a_{ij} \leq p_{ij} \leq M_{ij}a_{ij}, \quad -M_{ij}a_{ij} \leq q_{ij} &\leq M_{ij}a_{ij}, \end{aligned}$$

where M_{ij}, N_{ij} are chosen to be sufficiently large positive numbers. They are chosen such that $M_{ij} > \left|G_{ij}c_{ij} + B_{ij}s_{ij} - G_{ij}e_i\right|$ and $N_{ij} > \left|(B_{ij} - b_{ij}/2)e_i - B_{ij}c_{ij} + G_{ij}s_{ij}\right|$. Note that an alternative approach to the big-M method is to use convex hull reformulations of these constraints to represent the feasible set [35].

We need to ensure that only lines with either switches or circuit breakers can be opened. Suppose SW is an $n \times n$ matrix that indicates whether a line has a switching device, i.e., $SW_{ij} = 1$ and is 0 otherwise. Then, the following constraint ensures that only valid switching actions are allowed:

$$1 - a_{ij} \leq SW_{ij} \quad \forall (i,j) \in L. \tag{59}$$

Finally, we can optionally add an upper limit on the total number of lines that can be opened in the optimized network:

$$\sum_{(i,j)\in L} (1 - a_{ij}) \leq N_{sw}.$$

This allows the grid operator to control exactly how many switching operations can be made at each timestep. This may be necessary for real systems where it may not be feasible to operate all available switches and circuit breakers. Thus, we have relaxed the original nonconvex mixed integer nonlinear program for OTS-ACOPF to a mixed integer second-order conic convex program (MISOCP)—these are much more computationally tractable to solve than MINLPs.

3. Numerical Simulations and Results

We now briefly present some simulations of the proposed formulations on a few different IEEE standard transmission test cases. We conduct studies for the IEEE 9-bus, 39-bus, and 118-bus systems, all of which are meshed networks. These are relatively small networks, but they still demonstrate some interesting results that we summarize below. Here, we provide some notes on the simulations themselves:

- For the larger systems, there were several cases where the solver had difficulties converging to the optimal solution or reported local infeasibility. This was especially a challenge for the MINLP formulations and/or while using free solvers like IPOPT or SCIP.
- In order to deal with this, we warm-started the optimization process by initializing the variables using solutions from DCOPF, more relaxed versions of the same problem, or by temporarily removing certain constraints like the line flow limits. This enabled achieving convergence for all the cases.
- For simplicity, we used a fixed large value of $M = 100$ for the big-M relaxations. This worked well, since we already know most of our variables and terms are of the order of ≈ 1.0 after per-unitization. However, tuning the value of M for different cases could improve the performance and also avoid potential issues around ill-conditioning and scaling (although, this did not occur during our simulations).

All the network parameters and nodal load data are the default values specified in the respective IEEE test case datasheet from the Texas A&M Electric Grid Test Case Repository [36] and were taken from the MATPOWER library [29]. The problem was modeled using the JuMP optimization framework in Julia [37], and all the formulations except the nonconvex ACOPF were solved using Gurobi. The nonconvex ACOPF was solved using the IPOPT solver. The simulations were run on a 2021 MacBook Pro M1 Max with 64 GB RAM. The results are summarized in Tables 2 and 3.

Table 2. Computational comparison of different OPF and OTS approaches. For a fair comparison, these were all solved using the free open-source SCIP solver in Julia.

Runtime (s)	9-Bus	39-Bus
Different OPF formulations		
(1) DC OPF	0.0033	0.0061
(2) Non-convex AC OPF	0.0249	0.744
(3) SOCP relaxed OPF	0.045	0.639
(4) SOCP relaxed OPF + MCEs	0.0556	0.677
OTS simulations with no constraints on switching actions N_{sw}		
(5) DC OPF OTS	0.0575	0.555
(6) Non-convex ACOPF OTS	0.0806	0.376
(7) OTS with SOCP relaxation + bilinear terms	0.0728	0.402
(8) OTS with SOCP relaxation + Big-M reformulations	0.0437	0.387
(9) MISOCP relaxed OTS with Big-M + MCEs	0.0815	0.527

Table 3. Optimality comparison of different OPF and OTS approaches.

Optimality Gap (%)	9-Bus	39-Bus
Different OPF formulations		
(1) DC OPF	0.0891	1.091
(2) Non-convex AC OPF (exact)	0	0
(3) SOCP relaxed OPF	3.712×10^{-10}	1.955×10^{-14}
(4) SOCP relaxed OPF + MCEs	1.115×10^{-9}	4.671×10^{-12}
OTS simulations with no constraints on switching actions N_{sw}		
(5) DC OPF OTS	0.0891	0.024
(6) Non-convex ACOPF OTS	0	0
(7) OTS with SOCP relaxation + bilinear terms	7.71×10^{-7}	1.87×10^{-14}
(8) OTS with SOCP relaxation + Big-M reformulations	1.639×10^{-14}	2.307×10^{-12}
(9) MISOCP relaxed OTS with Big-M + MCEs	6.988×10^{-8}	8.906×10^{-10}

3.1. Comparisons of Different Formulations

We first compared the different formulations in terms of their computational performance, as shown in the table below. The formulations are defined as follows:

1. DC OPF: the simplest version of the problem, a convex quadratic program (with linear constraints).
2. Non-convex nonlinear AC OPF: exactly describes the power physics.
3. SOCP relaxed OPF: using second-order conic programming convex relaxation but still containing the nonconvex trigonometric voltage angle constraint.
4. SOCP relaxed OPF + MCEs: also relax the nonconvex trigonometric voltage angle constraints using a small angle approximation and McCormick envelopes (MCE).
5. (1) with OTS.
6. (2) with OTS.
7. (3) with OTS, containing bilinear terms involving products of binary and continuous variables.
8. (7) with big-M reformulations to remove the bilinear terms.
9. MISOCP by combining (8) with MCE relaxations of the angle constraint.

In this study, we focus only on the optimality gap and solution times as the two key measures of computational performance for each algorithm. However, it is important to note that other metrics could also be considered for a more rigorous comparison. We plan to analyze other aspects of each algorithm in future work. However, here we consider a

simplified analysis as a starting point since runtime and optimality are often the factors most important to decision makers like grid operators and utilities. Another important factor to consider is the feasibility gap, since the relaxed OPF or OTS solutions may not necessarily always be feasible for the exact OPF problem. However, we know that all of our proposed relaxed formulations (3), (4), and (6)–(9) are based on AC-power flow and thus will offer better feasibility guarantees than the DC approaches (1) and (5).

As expected intuitively, we see that the optimality gap in Table 3 increases as we further relax and approximate the problem. Here, we used the relative difference between optimal solution values to compare the gap between different formulations. The DC OPF (1) is significantly worse than all the other formulations, indicating that solutions from the DC OPF may not necessarily be optimal for the real system or may not even be AC feasible, since it does not take into account all the constraints. The other relaxations work reasonably well, although their exact performance depends on the specific test case being considered. For the nominal operation, the SOCP relaxed OPF (3) works best, and further convexifying the angle constraint via MCEs in (4) only marginally increases the optimality gap. This suggests that the MCE approach is valid at least for these test cases. In terms of the OTS formulations, we see that the final convex MISOCP formulation with MCEs (9) still has a relatively small optimality gap. One interesting point is that the big-M reformulation in (8) performs much better than (7) on the 9-bus case but worse on the 39-bus case. This will be investigated further as part of our future work.

The DC OPF is significantly faster than the other methods in most cases, owing to its simple model, but this comes at the cost of lower accuracy and we may need to check for the AC feasibility of the obtained solutions Interestingly, we find that some of the relaxations actually take slightly longer than their nonconvex stricter counterparts. This may be due to the additional variables we needed to introduce to deal with the nonlinearities, which increase the dimensionality. However, we expect that the relaxed formulations may scale better for larger networks. This hypothesis will be tested through more simulations in future work. Another encouraging trend from Table 2 is that the relaxations seem to offer more of an incremental benefit (in terms of faster solution times) when applied to the OTS problem to solve the MINLPs, as opposed to the nominal case without OTS where we are solving a simpler problem.

While we observed low optimality gaps with the relaxations for these experiments, this is not guaranteed for all situations. Further refinements can be made to restrict the feasible space, obtain tighter relaxations, and ensure that the obtained solutions are feasible for the original nonconvex program. Nevertheless, applying any of the above ACOPF-based relaxations would still offer better approximations than the crude DCOPF approximation.

3.2. Sensitivity Analysis for Selecting Big-M Value

We conducted a brief sensitivity analysis to understand the impacts of the big-M values on the run-time and conditioning of the power flow problem. This was achieved using the IEEE 9-bus, 39-bus, and 118-bus test cases, by running formulation (9) for the OTS problem, i.e., MISOCP relaxed OTS with Big-M constraints + MCEs (see Table 2). We estimated the problem conditioning by extracting the condition number of the constraint 'A' (left-hand side) matrix. We observed that while the problem conditioning is pretty stable and relatively insensitive to the big-M value, the run-time needed to solve the optimization problem is more significantly affected by the chosen big-M value. Looking across the sensitivity curves for the three test networks in Figure 1, we find that a value of around $M = 100$ generally works well across all three networks, in terms of the lowest average run times. These relatively low M values seem to work well for our application while also ensuring satisfactory feasibility and optimality levels. One reason for this may be because

all of our inputs, parameters, and decision variables have been normalized to per unit (p.u.) values, with small magnitudes generally of the order of 1. Although higher M values may potentially further reduce the runtime or improve strict feasibility, these come with the tradeoff of risking instability and ill-conditioning, especially for larger networks. As intuitively expected, we also see that the run-times consistently increase as we increase the network size, across all big-M values.

In general, the exact optimal value of M does depend on a variety of factors such as the system size, network density, the number of integer decision variables, etc. A more exhaustive big-M analysis for larger-scale problems will be considered in future work. For instance, one potential way to study the influence of the number of decision variables could be by varying the maximum number of lines with switches that can be opened at any given time, i.e., N_{sw}.

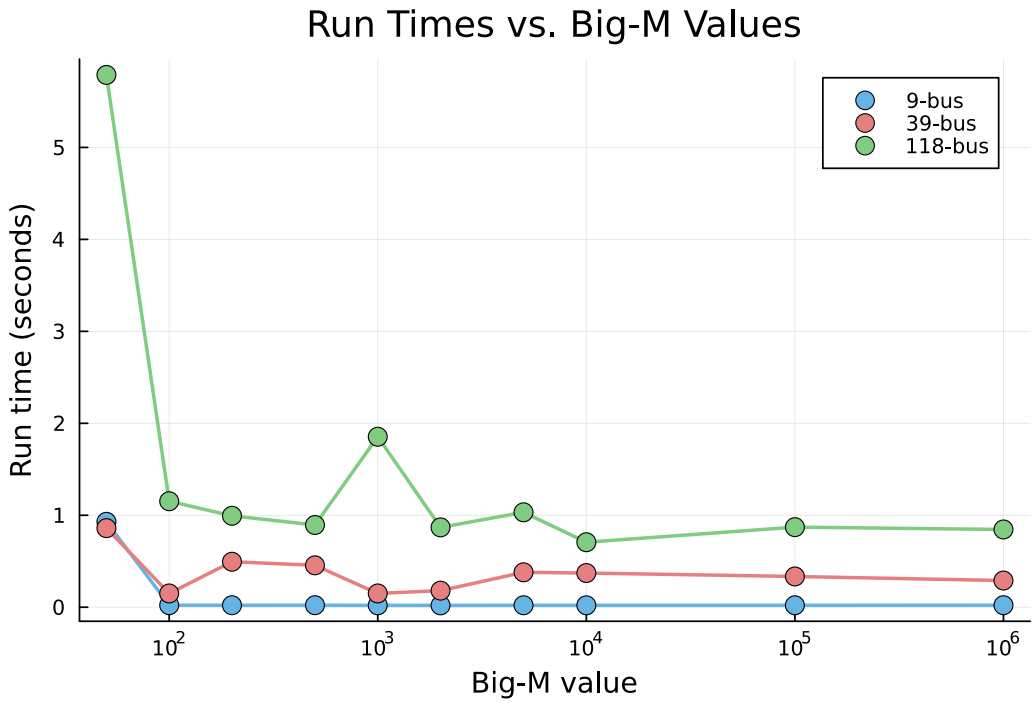

Figure 1. Run-time versus big-M value. The 3 different colored lines (and circle data points) denote the run-time results corresponding to each of the 3 networks tested in our simulations.

3.3. Effects of OTS on the System

Although we tested all nine formulations on the test cases, for conciseness, here, we only report the results for (i) the nominal case while applying approach (4) vs. (ii) the OTS case by applying (9) on the larger IEEE-118 bus system. We simulated the OPF dispatch using load and generation data for 1 h. This is because we did not observe significant impacts of OTS on the smaller 9-bus and 39-bus systems, indicating that they are not really transmission capacity-constrained. The IEEE-118 bus system consists of 19 generators, 35 synchronous condensers, 177 lines, nine transformers, and 91 loads, shown in Figure 2. These simulations were run using the Gurobi solver in Julia. We assessed the impacts of OTS by examining some important metrics. We can obtain the locational marginal prices (LMP) at each bus as the dual multipliers associated with the real power (P) balance constraints. These are how electricity prices are set in the wholesale market as well. The differences in LMPs across different buses in the network indicate that there is congestion, i.e., the network operation is constrained by the transmission capacity

of the lines (power flow limits). The effect of congestion on system performance can be quantified via the congestion rent:

$$\text{Congestion rent} = CR = \left(\sum_{i=1}^{n_D} p_D^i \cdot LMP_i\right) - \left(\sum_{j=1}^{n_G} p_j^G \cdot LMP_j\right).$$

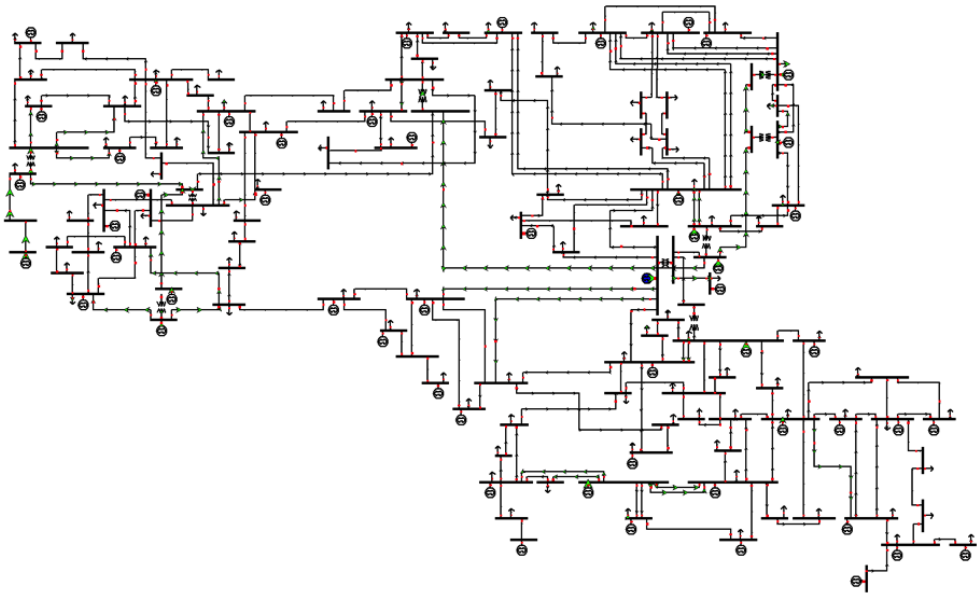

Figure 2. IEEE-118 bus system.

This is the difference between the total amount paid by electricity consumers minus the costs of procuring it from the generators; thus, $CR > 0$ indicates that there are inefficiencies in the market allocation due to the effects of congestion and losses. Another key metric is the total system-wide cost of meeting the demand, given by the total generation cost. This can be directly queried as the objective function value at the optimal solution:

$$\sum_{i \in G} f_i(P_{Gi}^*) = \sum_{i \in G} C_i^{G1}\left(p_i^G\right)^2 + C_i^{G2} p_i^G + C_i^{G13},$$

where we used a quadratic variable cost function, which is characteristic of conventional fossil fuel-based generators. Finally, we can quantify the extent to which the transmission capacity is constrained through the flowrate marginal prices (FMPs), which correspond to the dual variables of the line flow limit inequality constraints Equation (43). These are zero for lines that are not congested, since the constraint with strict inequality but screening for non-zero values allows us to identify which lines are congested and to what extent.

We find that applying OTS creates significant benefits, especially in terms of reducing system-wide congestion. This results in lower LMPs and FMPs and thus lower congestion rents. The main results in Table 4 highlight the effects of implementing OTS on the IEEE-118 bus test system. Improved dispatch allows us to shift some generation to cheaper sources, lowering the total costs slightly as well. The lower spatial volatility in LMPs also indicates lower congestion and more efficient network operation. For simplicity, these simulations were run with no constraint N_{sw}. Thus, it is important to note that these benefits may be less pronounced if there is an upper limit imposed by the operator on the number of lines allowed to be open or turned 'OFF' (N_{sw}).

Table 4. Effects of OTS on the IEEE-118 bus test system.

	Nominal	OTS
With no Limit on N_{sw}		
Total generation cost ($/h)	62,165	60,018 (−3.45%)
Congestion rent ($/h)	39,433	2579 (−93.45%)
Average LMP ($/MWh)	44.23	33.84 (−23.49%)
Average |FMP| ($/MWh)	0.7404	0.0176 (−97.62%)
LMP standard deviation ($/MWh)	11.89	0.775 (−93.49 %)
No. of congested lines	5	4
Optimal no. of open lines	N/A	32 (out of 186 total)

4. Conclusions and Future Work

In this study, we formulated and simulated various different optimal power flow relaxations and applied them to the optimal transmission switching problem. We built upon previous work to include more accurate models and constraints while performing OTS. In addition to comparing the runtime and performance of these approaches on three different realistic test networks, we also demonstrated the benefits of applying OTS on a larger system. It helps reduce overall costs and congestion and results in a more efficient power dispatch system-wide. For future work, we plan to scale up this approach to much larger transmission grids in order to more rigorously compare the different formulations. This will also allow us to assess what the true potential of OTS is. We would also like to consider OTS in the context of coordinated transmission and distribution grid operation [38,39]. Extensions to other operating conditions, like line faults and contingencies, will also be considered, where voltage magnitudes may deviate significantly from the nominal values.

Funding: This research received no external funding.

Data Availability Statement: All the data used in this study for the IEEE 9-bus, 39-bus, and 118-bus test systems are publicly available in the Electric Grid Test Case Repository from Texas A&M University, at https://electricgrids.engr.tamu.edu/electric-grid-test-cases/ (accessed on 18 February 2025) [36].

Conflicts of Interest: The authors declare no conflicts of interest.

References

1. Johnston, S.; Liu, Y.; Yang, C. *An Empirical Analysis of the Interconnection Queue*; Technical Report; National Bureau of Economic Research: Cambridge, MA, USA, 2023.
2. Lee, T.; Nair, V.J.; Sun, A. Impacts of dynamic line ratings on the ERCOT transmission system. In Proceedings of the 2022 North American Power Symposium (NAPS), Salt Lake City, UT, USA, 9-11 October 2022; pp. 1–6.
3. Fisher, E.B.; O'Neill, R.P.; Ferris, M.C. Optimal transmission switching. *IEEE Trans. Power Syst.* **2008**, *23*, 1346–1355. [CrossRef]
4. Hedman, K.W.; Oren, S.S.; O'Neill, R.P. A review of transmission switching and network topology optimization. In Proceedings of the IEEE Power and Energy Society General Meeting, Detroit, MI, USA, 24–28 July 2011. [CrossRef]
5. Numan, M.; Abbas, M.F.; Yousif, M.; Ghoneim, S.S.; Mohammad, A.; Noorwali, A. The Role of Optimal Transmission Switching in Enhancing Grid Flexibility: A Review. *IEEE Access* **2023**, *11*, 32437–32463. [CrossRef]
6. Hedman, K.W.; O'Neill, R.P.; Fisher, E.B.; Oren, S.S. Optimal transmission switching—Sensitivity analysis and extensions. *IEEE Trans. Power Syst.* **2008**, *23*, 1469–1479. [CrossRef]
7. Hedman, K.W.; O'Neill, R.P.; Fisher, E.B.; Oren, S.S. Optimal transmission switching with contingency analysis. *IEEE Trans. Power Syst.* **2009**, *24*, 1577–1586. [CrossRef]
8. Peker, M.; Kocaman, A.S.; Kara, B.Y. Benefits of transmission switching and energy storage in power systems with high renewable energy penetration. *Appl. Energy* **2018**, *228*, 1182–1197. [CrossRef]

9. Little, E.; Bortolotti, S.; Bourmaud, J.Y.; Karangelos, E.; Perez, Y. Optimal Transmission Topology for Facilitating the Growth of Renewable Power Generation. In Proceedings of the 2021 IEEE Madrid PowerTech, Madrid, Spain, 28 June–2 July 2021. [CrossRef]
10. Ruiz, P.A.; Rudkevich, A.; Caramanis, M.C.; Goldis, E.; Ntakou, E.; Philbrick, C.R. Reduced MIP formulation for transmission topology control. In Proceedings of the 2012 50th Annual Allerton Conference on Communication, Control, and Computing, Allerton, Monticello, IL, USA, 1–5 October 2012; pp. 1073–1079. [CrossRef]
11. Khanabadi, M.; Ghasemi, H.; Doostizadeh, M. Optimal transmission switching considering voltage security and N-1 contingency analysis. *IEEE Trans. Power Syst.* **2013**, *28*, 542–550. [CrossRef]
12. Jabarnejad, M. A genetic algorithm for AC optimal transmission switching. In *GECCO 2021, Proceedings of the 2021 Genetic and Evolutionary Computation Conference, Lille, France, 10–14 July 2021*; Association for Computing Machinery: New York, NY, USA, 2021; pp. 973–981. [CrossRef]
13. Bai, Y.; Zhong, H.; Xia, Q.; Kang, C. A Two-Level Approach to AC Optimal Transmission Switching with an Accelerating Technique. *IEEE Trans. Power Syst.* **2017**, *32*, 1616–1625. [CrossRef]
14. Nazemi, M.; Dehghanian, P.; Lejeune, M. A mixed-integer distributionally robust chance-constrained model for optimal topology control in power grids with uncertain renewables. In Proceedings of the 2019 IEEE Milan PowerTech, Milan, Italy, 23–27 June 2019. [CrossRef]
15. Li, X.; Xia, Q. Stochastic Optimal Power Flow with Network Reconfiguration: Congestion Management and Facilitating Grid Integration of Renewables. In Proceedings of the IEEE Power Engineering Society Transmission and Distribution Conference, Chicago, IL, USA, 12–15 October 2020. [CrossRef]
16. Mohseni-Bonab, S.M.; Kamwa, I.; Rabiee, A.; Chung, C.Y. Stochastic optimal transmission Switching: A novel approach to enhance power grid security margins through vulnerability mitigation under renewables uncertainties. *Appl. Energy* **2022**, *305*, 117851. [CrossRef]
17. Zhou, Y.; Zhu, H.; Hanasusanto, G.A. Distributionally Robust Chance-Constrained Optimal Transmission Switching for Renewable Integration. *IEEE Trans. Sustain. Energy* **2023**, *14*, 140–151. [CrossRef]
18. Henneaux, P.; Kirschen, D.S. Probabilistic security analysis of optimal transmission switching. *IEEE Trans. Power Syst.* **2016**, *31*, 508–517. [CrossRef]
19. Fuller, J.D.; Ramasra, R.; Cha, A. Fast heuristics for transmission-line switching. *IEEE Trans. Power Syst.* **2012**, *27*, 1377–1386. [CrossRef]
20. Crozier, C.; Baker, K.; Toomey, B. Feasible region-based heuristics for optimal transmission switching. *Sustain. Energy Grids Netw.* **2022**, *30*, 100628. [CrossRef]
21. Kocuk, B.; Dey, S.S.; Andy Sun, X.; Research, O.; Andy Sun Milton Stewart, X.H. Strong SOCP relaxations for the optimal power flow problem. *Oper. Res.* **2016**, *64*, 1177–1196. [CrossRef]
22. Kocuk, B.; Dey, S.S.; Sun, X.A. New Formulation and Strong MISOCP Relaxations for AC Optimal Transmission Switching Problem. *IEEE Trans. Power Syst.* **2017**, *32*, 4161–4170. [CrossRef]
23. Wu, X.; Conejo, A.J.; Amjady, N. Robust security constrained ACOPF via conic programming: Identifying the worst contingencies. *IEEE Trans. Power Syst.* **2018**, *33*, 5884–5891. [CrossRef]
24. Molzahn, D.K.; Dörfler, F.; Sandberg, H.; Low, S.H.; Chakrabarti, S.; Baldick, R.; Lavaei, J. A Survey of Distributed Optimization and Control Algorithms for Electric Power Systems. *IEEE Trans. Smart Grid* **2017**, *8*, 2941–2962. [CrossRef]
25. Molzahn, D.K.; Hiskens, I.A. A Survey of Relaxations and Approximations of the Power Flow Equations. *Found. Trends R Electr. Energy Syst.* **2019**, *4*, 1–221. [CrossRef]
26. Low, S.H. Convex relaxation of optimal power flow—Part i: Formulations and equivalence. *IEEE Trans. Control Netw. Syst.* **2014**, *1*, 15–27. [CrossRef]
27. Low, S.H. Convex relaxation of optimal power flow-part II: Exactness. *IEEE Trans. Control Netw. Syst.* **2014**, *1*, 177–189. [CrossRef]
28. Kundur, P. *Power System Stability and Control*; McGraw-Hill: New York, NY, USA, 1994.
29. Zimmerman, R.D.; Murillo-Sanchez, C.E.; Thomas, R.J. MATPOWER: Steady-State Operations, Planning, and Analysis Tools for Power Systems Research and Education. *IEEE Trans. Power Syst.* **2011**, *26*, 12–19. [CrossRef]
30. Wood, A.J.; Wollenberg, B.F.; Sheblé, G.B. *Power Generation, Operation, and Control*, 3rd ed.; Wiley: Hoboken, NJ, USA, 2013.
31. CIGRÉ Study Committee B4. Benchmarking of Control Strategies for HVDC Grids. Technical Report, 2009. Technical Brochure No. 379. Available online: https://www.cigre.org (accessed on 18 February 2025).
32. Islam, F.R.; Pota, H.R. Review of Power System Distribution Network Architecture. In Proceedings of the 2016 Australasian Universities Power Engineering Conference (AUPEC), Brisbane, QLD, Australia, 25–28 September 2016; pp. 1–6. [CrossRef]
33. *ANSI C84.1-2020*; American National Standard for Electric Power Systems and Equipment—Voltage Ratings (60 Hertz). American National Standards Institute: Washington, DC, USA, 2020. Available online: https://www.nema.org/standards/view/American-National-Standard-for-Electric-Power-Systems-and-Equipment-Voltage-Ratings (accessed on 18 February 2025).
34. Castro, P.M. Tightening piecewise McCormick relaxations for bilinear problems. *Comput. Chem. Eng.* **2015**, *72*, 300–311. [CrossRef]

35. Nagarajan, H.; Sundar, K.; Hijazi, H.; Bent, R. Convex hull formulations for mixed-integer multilinear functions. *AIP Conf. Proc.* **2019**, *2070*, 20037.
36. Kunkolienkar, S.; Safdarian, F.; Snodgrass, J.; Birchfield, A.; Overbye, T. A Description of the Texas A&M University Electric Grid Test Case Repository for Power System Studies. In Proceedings of the 2024 IEEE Texas Power and Energy Conference (TPEC), College Station, TX, USA, 12–13 February 2024; pp. 1–6. [CrossRef]
37. Dunning, I.; Huchette, J.; Lubin, M. JuMP: A modeling language for mathematical optimization. *SIAM Rev.* **2017**, *59*, 295–320. [CrossRef]
38. Li, Z.; Guo, Q.; Sun, H.; Wang, J. Coordinated transmission and distribution AC optimal power flow. *IEEE Trans. Smart Grid* **2018**, *9*, 1228–1240. [CrossRef]
39. Lin, C.; Wu, W.; Shahidehpour, M. Decentralized AC Optimal Power Flow for Integrated Transmission and Distribution Grids. *IEEE Trans. Smart Grid* **2020**, *11*, 2531–2540. [CrossRef]